

Document downloaded from:

<http://hdl.handle.net/10251/72944>

This paper must be cited as:

Gamboa-Santos, J.; Montilla, A.; Carcel Carrión, JA.; Villamiel, M.; García Pérez, JV. (2014). Air-borne ultrasound application in the convective drying of strawberry. *Journal of Food Engineering*. 128:132-139. doi:10.1016/j.jfoodeng.2013.12.021.



The final publication is available at

<https://dx.doi.org/10.1016/j.jfoodeng.2013.12.021>

Copyright Elsevier

Additional Information

14 **Abstract**

15 The use of non-thermal technologies, such as power ultrasound, is mostly suitable for
16 the drying of thermolabile food materials. Thereby, the air-borne ultrasonic application as a
17 means of improving the convective drying of strawberry has been explored in this work.
18 Experiments were conducted by setting the acoustic power applied (0, 30 and 60 W) and the
19 air temperature (40, 50, 60 and 70 °C). The desorption isotherms and the shrinkage pattern
20 were also experimentally determined. In order to describe the drying kinetics, a diffusion
21 model considering both convective transport and shrinkage was used.

22 The increase in both the applied acoustic power and temperature gave rise to a
23 significant reduction of drying time (13-44%). The application of power ultrasound involved
24 a significant ($p<0.05$) improvement in the effective moisture diffusivity and the mass transfer
25 coefficient, the effect being less intense at high temperatures. The results reported here
26 highlight the fact that ultrasonic application during convective drying is a promising
27 supporting technology with which to reduce the drying time needed for heat sensitive
28 products, such as strawberry.

29

30 Key-words: Non-thermal processing; ultrasound; strawberry; modeling; effective
31 diffusivity; mass transfer coefficient

32

33 1. Introduction

34 Over many decades, convective drying using hot air has been considered as the
35 conventional dehydration method for foodstuffs since it extends shelf life and makes the low
36 cost transportation and storage of the dry material easier. Despite being the most widely-
37 addressed technique, hot air drying is considered one of the most energy intensive industrial
38 operations. Thus, it is estimated that thermal dehydration processes account for up to 25% of
39 the industrial energy consumption in developed countries (Chen & Mujumdar, 2008).

40 In order to understand the drying process and be able to improve it, mass transfer
41 phenomena have been studied and the controlling resistances taken into account (Bon et al.,
42 2007; Giner, 2009; Ozuna et al., 2011; Barati & Esfahani, 2013). Water transfer is mainly
43 controlled by the rate of the water movement inside the materials (internal resistance, IR) and
44 the convective transport from the solid surface to the air (external resistance, ER). The
45 internal resistance is characteristic of the food material, while the external one depends
46 mostly on the thickness of the diffusion boundary layer (Cárcel et al., 2007). Despite the great
47 efforts made to improve the drying process, it is known that optimal requirements for the heat
48 and mass transfer do not necessarily ensure the final products are of optimal quality.

49 During hot air drying, product quality loss is linked to the use of high temperatures and
50 long drying times. Thus, the limitations to a conventional drying process could be partially
51 overcome by using additional energy sources, such as microwave (Li et al., 2011), infrared
52 radiation (Rastogi, 2012) or power ultrasound (US) (Cárcel et al., 2012; Chandrapala et al.,
53 2012), which should help to reduce both drying time and temperature. In the case of
54 microwave or infrared radiation, there is a risk of product overheating, which has to be
55 considered when the drying of heat-sensitive products is addressed. On the contrary, US
56 waves mainly produce mechanical effects and their air-borne application can intensify the
57 water removal without introducing a high amount of thermal energy during drying (Riera et

58 al., 2011). This represents a great improvement in the field of non-thermal processing and
59 environmentally-friendly, energy-saving technologies. In fact, it is acknowledged that US
60 technology is a good example of how to ensure sustainability (Gallego-Juárez, 2010).
61 Moreover, the fact that applying power US in gas media only produces a low thermal effect
62 means that its application in the drying of heat-sensitive materials is of interest (Awad et al.,
63 2012; Cárcel et al., 2012; Chemat et al., 2011). The ultrasonic effects in gas-solid systems are
64 mainly linked to the rapid series of alternative compressions and expansions promoted by the
65 ultrasonic waves in both the solid particle (“sponge effect”) and the surrounding air. This
66 mechanical force can create microscopic channels that allow an easier inner water movement
67 (De la Fuente-Blanco et al., 2006), as well as microstreaming and high turbulence at the
68 interfaces (Cárcel et al., 2012). Additionally, the phenomenon of cavitation could provoke the
69 removal of the most strongly attached water molecules (Soria & Villamiel, 2010). Recent
70 studies have reported how air-borne US application in food drying is greatly affected by both
71 the operational parameters and product properties (Ozuna et al., 2011). These studies have
72 addressed the US application in the drying of lemon (García-Pérez et al., 2009) and orange
73 peel (Ortuño et al., 2010; García-Pérez et al., 2012), olive leaves (Cárcel et al., 2010),
74 potatoes (Ozuna et al., 2011) and carrots (Cárcel et al., 2011), among others. However, to the
75 best of our knowledge, there have been no previous studies into the ultrasonically assisted
76 convective drying of berries. Strawberries are fruits which enjoy wide consumer acceptance
77 not only due to their palatability but also to their nutritive value and bioactivity (Giampieri et
78 al., 2012), making strawberries one of the largest fruit crops (Doymaz, 2008).

79 The aim of this paper was to assess the influence of the air temperature and the
80 application of ultrasound on the convective drying kinetics of strawberry. For that purpose,
81 experimental results were analyzed and modeled using the diffusion theory

82

83 2. **Materials and Methods**

84 2.1. *Samples preparation*

85 Fresh strawberries (*Fragaria x ananassa Duch*) were purchased from a local market in
86 Valencia (Spain) and stored at 5 °C for a maximum of 3 days until drying. After washing in
87 tap water, draining with blotting paper and removing the external impurities, strawberries
88 were cut into 2.5 ± 0.5 mm thick slices along their longitudinal axis.

89

90 2.2. *Moisture content*

91 The moisture content of fresh strawberries was determined at 70 °C and 80 mbar
92 vacuum level until constant weight (AOAC, 1990c).

93

94 2.3. *Airborne US dryer*

95 Strawberries were dried by using an ultrasonic-assisted convective dryer (**Figure 1**).
96 The prototype was initially a current pilot-scale convective dryer, with its drying chamber
97 subsequently modified to generate US waves (García-Pérez et al., 2006a; Riera et al., 2011).
98 The ultrasonic device includes a cylindrical vibrating radiator driven by a piezoelectric
99 transducer (21.8 kHz), which generates a high-intensity ultrasonic field in the air medium,
100 where the samples are placed. A high power US generator, an impedance matching unit and a
101 digital power meter (WT210, Yokogawa Electric Corporation, Japan) regulate and measure
102 the electrical parameters of the acoustic signal (voltage, intensity, phase, frequency and
103 power). The air parameters (velocity and temperature) were controlled through a PID
104 algorithm and a PC supervised the whole drying process.

105

106 2.4. *Drying experiments*

107 An air velocity of 2 m/s was chosen for drying experiments of strawberry slabs,
108 according to previous studies carried out in the same dryer (Cárcel et al., 2007; García-Pérez
109 et al., 2006a and 2009). The temperature ranged between 40 and 70 °C (**Table 1**), which
110 could be considered mild drying temperatures. Two levels of ultrasonic energy were set by
111 applying specific electric powers to the transducer (30 and 60 W). Convective drying
112 experiments were run under the same experimental conditions but without applying US (0
113 W), thus being denominated “nonUS” drying experiments in the following sections. At least
114 three replicates of each experimental condition were carried out. A summary of the
115 processing conditions tested is shown in **Table 1**.

116 In the drying experiments, samples (73.5 ± 3.5 g) were randomly distributed in the
117 drying chamber to minimize the influence of the heterogeneity of the generated acoustic field.
118 For that purpose, samples were placed inside the vibrating chamber suspended in a metallic
119 frame that allows free air flow around each individual piece. Sample weight was
120 automatically recorded at 3 min intervals during the whole drying process.

121

122 2.5. *Desorption isotherm*

123 The water desorption isotherms were obtained from fresh strawberries. Milled
124 samples (3.08 ± 0.05 g) were partially dehydrated in a conventional air-forced oven at 50 °C
125 for different times (from 0.5 to 17 h). This allowed obtaining samples with a wide range of
126 final water content (0.2-11.2 kg water (W)/kg dry matter (DM)). The partially dried samples
127 were kept at 25 °C for 24 h in closed containers to achieve a homogeneous moisture
128 distribution. Then, the water activity (a_w) was measured in a standardized conductivity

129 hygrometer NOVASINA TH-500 (Air Systems for Air Treatment, Pfäffikon, Switzerland) at
130 25 °C. The device was previously calibrated using the following salts: LiCl, MgCl₂,
131 Mg(NO₃)₂, NaCl, BaCl₂ and K₂Cr₂O₇ following the calibration procedure of the equipment
132 manufacturer. Once a_w was determined, the sample moisture content was measured in
133 triplicate (AOAC, 1990c). A total number of 30 water activity/moisture content experimental
134 points were obtained. The well-known Brunauer, Emmet and Teller sorption isotherm model
135 (Brunauer et al., 1938) was the equation used to describe the relationship between
136 experimental a_w and moisture (Eq. 1). The BET model was fitted to the experimental data by
137 using the SOLVER optimization tool available in Microsoft EXCELTM, identifying the model
138 parameters (the monolayer moisture content, W_m , and the energy constant, C), which
139 minimized the sum of the squared difference between the experimental and calculated
140 moisture content.

$$W = W_m \frac{Ca_w}{(1 - a_w)(1 + (C - 1)a_w)} \quad (1)$$

141 where W is the average moisture content (kg W/kg DM), a_w the water activity, W_m the
142 monolayer moisture content (kg W/kg DM) and C the BET's model parameter
143 (dimensionless).

144

145 2.6. Determination of Shrinkage

146 The product shrinkage was estimated using cubic samples of strawberries (8.5 mm),
147 dried at 70 °C using an air velocity of 2 m/s and without US application (0 W). This kind of
148 sample was chosen assuming an isotropic shrinkage and in order to improve the accuracy of
149 the estimation. For that purpose, during drying, three samples were randomly collected and
150 weighed every 30 min, measuring their moisture content (AOAC, 1990c) and volume. The

151 toluene displacement method was used to measure the volume (toluene density 0.867 g/mL at
152 20 °C) using a volumetric standard picnometer (48.89 mL) and an analytical balance (PB
153 303-5, Mettler Toledo) (García-Pérez et al., 2011). From the measurement of the volume, the
154 length of the mass transport characteristic dimension (L), which coincides with the half-
155 length of the cube side, was calculated by considering the samples maintained their cubic
156 geometry. The relationship between L and the moisture content was considered in the mass
157 transport modeling.

158

159 2.7. *Modeling the drying kinetics*

160 The diffusion theory was considered to describe the one-dimensional water transfer
161 during drying. The governing equation (Eq. 2) for infinite slab geometry takes into account
162 both the solid isotropy and a constant effective moisture diffusivity (D_e) during drying
163 (Simal et al., 2003).

$$\frac{\partial W_p(x,t)}{\partial t} = D_e \frac{\partial^2 W_p(x,t)}{\partial x^2} \quad (2)$$

164 where W_p is the local moisture content (kg W/kg DM), x the mass transport direction (m) and
165 t the time (s).

166 The model solution was addressed by considering that the sample volume did not
167 remain constant during drying due to the phenomenon of shrinkage, which is especially
168 noticeable in high-porosity products, such as fruits and vegetables (Schössler et al., 2012).
169 Thus, mass transport was addressed as a moving boundary problem considering the half
170 length of the infinity slab (L , m) to be moisture dependent, which was experimentally
171 determined as explained before. For initial and boundary conditions, a homogeneous
172 moisture content distribution in the solid (Eq. 3) and the solid symmetry (Eq. 4) was

173 considered. Moreover, the external resistance (ER) to mass transfer was taken as significant
 174 (Eq. 5) due to the low air velocity used, as reported in literature in previous studies (García-
 175 Pérez et al., 2009).

$$t = 0 \quad W_p(x, 0) = W_0 \quad (3)$$

$$t > 0; x = 0 \quad \frac{\partial W_p(0, t)}{\partial x} = 0 \quad (4)$$

$$t > 0; x = L \quad -D_e \rho_{ds} \frac{\partial W_p(L, t)}{\partial x} = k(a_w(L, t) - \varphi_{air}) \quad (5)$$

176

177 where ρ_{ds} is the dry solid density (kg DM/m³), k is the mass transfer coefficient (kg
 178 W/m²/s), a_w is the water activity on the solid surface and φ_{air} is the relative humidity of the
 179 drying air.

180 Experimental sorption isotherm (Eq. 1) at 25 °C was used to roughly estimate the water
 181 activity (a_w) at the sample surface (Eq. 5) for the different drying conditions tested. While,
 182 the experimentally estimated shrinkage pattern contributed to model the reduction of the
 183 characteristic dimension (L) during drying. Eq. (2) was solved by considering both the initial
 184 and the boundary conditions already depicted and by applying an implicit finite difference
 185 method (Mulet et al., 2005). For that purpose, a programming code was written in Matlab R
 186 2009d (The MathWorks, Inc., Natick, MA), which provided the local moisture distribution in
 187 the slab as well as the average moisture content (W). The model was fitted to the
 188 experimental drying kinetics by using the optimization tool *fminsearch function* (SIMPLEX
 189 method) available in Matlab. Thus, the D_e and k were simultaneously identified by
 190 minimizing the sum of the squared differences between the experimental and the calculated
 191 average moisture content.

192 In order to evaluate the fit of the models, the explained variance (VAR) and the mean
193 relative error (MRE) were computed from Eqs. (6) and (7) (Cárcel et al., 2011).

$$VAR = \left[1 - \frac{S_{tw}^2}{S_w^2} \right] \times 100 \quad (6)$$

$$MRE = \frac{100}{N} \left[\sum_{i=1}^N \frac{|W_{expi} - W_{calci}|}{W_{expi}} \right] \quad (7)$$

194
195 where S_w^2 and S_{tw}^2 are the variance of the experimental moisture data and the estimation,
196 respectively, W_{expi} and W_{calci} are the experimental and calculated average moisture contents
197 and N is the number of experimental data.

198 The Arrhenius equation was used (Sablani & Rahman, 2008) in order to quantify the
199 influence of the temperature on the D_e values (Eq. 8).

$$D_e = D_0 \exp\left(\frac{-E_a}{RT}\right) \quad (8)$$

200
201 Where D_0 is the pre-exponential Arrhenius factor (m^2/s), E_a is the activation energy (kJ/mol),
202 R is the universal gas constant (kJ/mol/K) and T is the temperature (K).

202 Analysis of variance (ANOVA) (Statgraphics 5.1 software) was carried out to identify
203 the significance (95%) of the influence of US application and air temperature factors on D_e
204 and k , while, Least Significance Intervals (LSD) were determined to identify significant
205 differences in the means.

206

207

208 3. **Results and discussion**

209 3.1. *Experimental drying data*

210 The strawberries presented an average initial moisture content of 9.55 ± 0.27 kg W/kg
211 DM, which was considered as the critical moisture content due to the lack of a constant rate
212 period under these experimental conditions. **Figure 2** shows the effect of temperature and
213 power US on the experimental drying kinetics.

214 The temperature increase gave rise to substantially shorter drying times, which was
215 noticeable at all the US powers applied. Thus, in order to reach an average moisture content
216 of 0.3 kg W/kg DM, samples dried without applying US (0 W) at 40, 50, 60 and 70 °C
217 needed 5.3, 4.6, 4.4 and 3.3 h, respectively. In the case of ultrasonically assisted drying
218 assays at 60 W, the drying times ranged from 4.6 h at 40 °C to 2.2 h at 70 °C.

219 As can be observed in **Figure 2**, not only the temperature, but also the application of
220 US affected the drying kinetic. At every temperature tested, the use of US improved the
221 drying rate, and the higher the ultrasonic power applied, the faster the drying. Thus, for
222 example, at 60 °C, the drying time needed to reach a moisture content of 0.3 (kg W/kg DM)
223 was reduced from 4.4 h (0 W) to 2.5 h by applying an ultrasonic power of 60 W. Average
224 drying time reductions brought about by applying US ranged from 13 to 44%. García-Pérez
225 et al. (2009), Ortuño et al. (2010), Ozuna et al. (2011) and Cárcel et al. (2011) reported
226 drying time reductions of about 30% in carrots, 53% in lemon peel, 45% in orange peel and
227 40% in potatoes under the same drying conditions (40 °C, 1 m/s and ultrasonic powers of up
228 to 90 W). Even more substantial drying time reductions have been found in the case of
229 eggplant, in which the application of an ultrasonic power of 90 W gave rise to a decrease of
230 72% in the drying time (García-Pérez et al., 2011). The internal structure of the different
231 products could be the reason for the difference observed. Thus, eggplant has a highly

232 unconsolidated tissue with a porous structure (Wu et al., 2007), which, consequently, is more
233 heavily influenced by US application than other vegetables and fruits, such as strawberry.

234 Despite there being no previous references to air-borne US application in strawberry
235 drying, García-Noguera et al. (2010) reported the osmotic dehydration of strawberry assisted
236 by US as a pretreatment in order to improve the effectiveness of the subsequent drying. These
237 authors found that the drying time of strawberry halves was shortened by about 50% when
238 the samples were previously treated with US (25 kHz) in a 50% sucrose solution (30 °C for
239 30 min) prior to drying (60 °C, 0.5 m/s and 16% air relative humidity). In the same study,
240 they also tested the ultrasonic pre-treatment in distilled water, which resulted in a reduction in
241 the air-drying time of 18% as compared to the untreated samples. In this case, the US effects
242 are linked to structural changes in the fruit tissue brought about mainly by the cavitation
243 produced in liquid media. Among other factors, it was reported that US increased the sucrose
244 added to strawberry, changing, therefore, the nature of the fresh product and so, the drying
245 behavior.

246

247 3.2. *Shrinkage*

248 Under the experimental conditions here assayed, it was assumed that the US application
249 and the different air temperatures did not significantly affect the shrinkage; thus, this
250 phenomenon was monitored during the drying of strawberries at 70 °C in nonUS assays. As
251 previously mentioned in the *Materials and Methods* section, assuming the isotropy of the
252 material, strawberry cubes of 8.5 mm were used in order to assess the change of the side
253 length from the measurement of the total volume. From experimentally obtained results, a
254 linear relationship was obtained between volume (V/V_0) and moisture ratios (W/W_0) (**Figure**
255 **3**). According to the literature, similar relationships have been reported describing the

256 shrinkage in other vegetables and fruits (Koc et al., 2008; García-Pérez et al. 2011). Thus, the
257 slope value (0.692) of this relationship (**Figure 3**) for strawberry drying was in the range
258 previously reported by Ramallo & Mascheroni (2013) for pineapple samples dried at
259 temperatures of between 45 and 75 °C (0.652-0.785). However, these values were lower than
260 those found in the drying of eggplant (0.929-0.960) using hot air (García-Pérez et al., 2011)
261 and a halogen moisture analyzer at 70-90 °C (Aversa et al., 2011). These differences might be
262 linked to the different product structure and drying method, which can affect the collapse of
263 the cell matrix.

264 From the afore-mentioned relationship, Eq. 9 was obtained to determine the change of
265 the characteristic diffusion dimension (L) during drying and, afterwards, included in the
266 modeling of the drying kinetics to provide a more realistic estimation of the effective
267 moisture diffusivity.

$$L = \sqrt[3]{(0.692 \frac{W}{W_0} + 0.325)L_0^3} \quad (9)$$

268 where subscript 0 refers to the initial time.

269

270 3.3. Desorption isotherms

271 The experimental desorption isotherm of strawberry determined at 25 °C is shown in
272 **Figure 4**. According to Brunauer's classification (Brunauer et al., 1940), it may be classified
273 as type III "Raoult's type" (Blahovec & Yanniotis, 2010): products with small amounts of
274 water at low a_w and large amounts at high a_w levels (García-Pérez et al., 2008). Type III
275 curves were also observed for other fruits (Lim et al., 1995; Mäskan & Gögüs, 1998;
276 Vázquez et al., 1999).

277 The BET model was used for modeling the experimental relationship between the a_w
278 and the equilibrium moisture content in strawberry samples. Despite the high experimental
279 variability observed, the BET model reached high VAR (96.3%) and low RME (9.4%). The
280 accuracy of the model's fit is also shown in **Figure 4**. The BET parameters identified from
281 modeling the experimental data of the a_w and the moisture content in strawberry samples
282 were 0.316 kg W/kg DM for W_m and 3.63 for C . The W_m value was slightly higher than those
283 reported for cherries and blueberries by Yu et al. (1998) (0.12-0.13 kg W/kg DM) and Vega-
284 Gálvez et al. (2009) (0.08-0.13 kg W/kg DM), but lower (0.74-0.95 kg W/kg DM) than others
285 reported for strawberries (Moraga et al., 2004). In the case of the C value, Garau et al. (2006),
286 García-Pérez et al. (2008) and Molina-Filho et al. (2011) obtained similar data when studying
287 orange peel (2.4), lemon peel (1.4-4.9) and pumpkins (1.9-4.2), respectively. Since parameter
288 C is related to water molecule-food matrix interactions (Erbaş et al., 2005), the results
289 obtained working on strawberries could be associated with a relatively low heat of sorption,
290 compared with values reported by Vega-Gálvez et al. (2009) for blueberries (C : 101.45 at 40
291 °C). In some of the previously-cited works (Moraga et al., 2004; Garau et al., 2006; García-
292 Pérez et al., 2008), GAB equations were simplified to BET models due to the fact that the K
293 constant of the GAB model was nearly equal to one; thus, they were used for the purposes of
294 comparison with the BET model parameters identified in this work.

295 The BET model here proposed will be used in the following section in the modeling of
296 the drying kinetics; it will help to quantify the convective water flux at the interface (Eq. 5).

297

298 3.4. Mass transport

299 **Table 2** shows the average effective moisture diffusivities (D_e) and the mass transfer
300 coefficients (k) identified from fitting the diffusion model for slab geometry to the

301 experimental drying kinetics of strawberry. The diffusion model, considering ER to mass
302 transfer and shrinkage to be significant, provided an accurate description of experimental
303 data. Regardless of the drying conditions, the obtained VAR values were over 99% and, in
304 overall terms, the MRE were under 5%. Moreover, **Figure 5** illustrates, taking as an example
305 the tests carried out at 70 °C (0, 30 and 60 W), the agreement between experimental and
306 calculated data by the model.

307 The D_e values (from 0.763 to $2.293 \times 10^{-10} \text{ m}^2/\text{s}$) shown in Table 2 were within the
308 same order of magnitude of others previously reported for the convective drying of
309 strawberries and also fell within the common range for foodstuffs (between 10^{-11} and 10^{-9})
310 (Doymaz, 2008). Furthermore, D_e values were close to those identified by García-Pérez et al.
311 (2009 and 2012); Ozuna et al. (2011) and Cárcel et al. (2011) in the US-assisted drying of
312 several fruits and vegetables.

313

314 *3.4.1. Effect of temperature*

315 As can be observed in **Table 2**, a rise in the drying temperature increased both the D_e
316 and k parameters at every ultrasonic power level tested. From 40 °C to 70 °C, the D_e and k
317 value were duplicated in both nonUS and US experiments. Similar results were obtained by
318 Doymaz (2008) for the convective drying of strawberries between 50 and 65 °C (D_e from
319 4.95×10^{-10} to $1.09 \times 10^{-9} \text{ m}^2/\text{s}$). D_e values reported by Doymaz (2008) were identified using
320 a diffusion model which did not consider ER, thus, in a certain way, they also include the
321 effect of temperature on external mass transport coefficients. Therefore, their direct
322 comparison with the results reported here is complicated. If models that consider ER to mass
323 transfer are taken into account, greater improvements in D_e have been identified. Thus, when
324 drying carrot cubes, García-Pérez et al. (2006b) reported a D_e increase of 137% when the

325 temperature rose from 40 °C ($1.93 \times 10^{-10} \text{ m}^2/\text{s}$) to 70 °C ($4.57 \times 10^{-10} \text{ m}^2/\text{s}$). The temperature
326 increase activates water molecules, speeding up the water transfer through the particle.

327 The influence of temperature on D_e was quantified from an Arrhenius type relationship
328 (Simal et al., 2005; Sablani & Rahman, 2008; Vega-Gálvez et al., 2008) (**Figure 6**). Linear
329 correlation coefficients higher than 0.99 were found for the different assays carried out (0, 30
330 and 60 W). The E_a value calculated ($25.3 \pm 1.9 \text{ kJ/mol}$) in nonUS experiments (0 W) was
331 within the range of those proposed for other products: 42.3 kJ/mol for peas (Senadeera et al.,
332 2003); 28.4 kJ/mol for carrots (Doymaz, 2004); 21.9 and 32.3 kJ/mol for kiwi (Simal et al.,
333 2005); 28.6-31.5 kJ/mol for papaya (Vega-Gálvez & Lemus-Mondaca, 2006), and 18.1- 43.2
334 kJ/mol for apple (Vega-Gálvez et al., 2008). The identified E_a values decreased to 21.9 ± 2.1
335 and $20.6 \pm 1.8 \text{ kJ/mol}$ for assays carried out applying 30 and 60 W respectively, as observed
336 in the slopes of the linear relationships depicted in **Figure 6**. Thus, E_a values for nonUS and
337 60 W experiments were significantly different ($p < 0.05$). Therefore, in a certain way, the
338 ultrasonic power affected the strawberry drying, this aspect being addressed in the following
339 section.

340

341 *3.4.2. Effect of power ultrasound*

342 The application of US increased the identified D_e and k values at every temperature
343 tested (**Table 2**), the effect being dependent on the power applied; so, the higher the power
344 applied, the larger the improvement of these parameters. In the case of D_e , the average
345 increase was of 18 and 42% for 30 and 60 W, respectively. Similar improvements were
346 reported for the US-assisted drying of other fruits and vegetables. Thus, in potatoes, the D_e
347 values increased by 19% (30 W) and 41% (60 W), when dried at 40 °C (Ozuna et al., 2011).
348 In the case of carrots, an increase of only 17% was obtained by applying 60 W at 40 °C

349 whereas average improvements of 62% and 100% were reported in lemon peel slabs dried at
350 40 °C and at 30 W and 60 W (García-Pérez et al., 2009). When studying other more porous
351 materials such as eggplant, García-Pérez et al. (2011) reported improvements of up to 92 and
352 211%, by applying US at 30 and 60 W, respectively. As reported in the literature (Riera et al.,
353 2011), the phenomenon of alternating expansion and contraction cycles produced by applying
354 power US to the materials should be what mainly speeds up the inner water movement, which
355 is manifested in the increase in D_e .

356 As already mentioned, the air temperature during drying influenced the effects of US
357 on mass transport. Thus, the average improvement of D_e at low temperatures (40, 50 °C) was
358 25.8 and 52.3% at 30 and 60 W, respectively, which was reduced to 11.1 and 31.5% at high
359 temperatures (mean for 60 and 70 °C, respectively). Likewise, the negative effect that high
360 temperatures have on the influence of US has also been reported in the case of carrot cube
361 drying (García-Pérez et al., 2006b). This phenomenon is linked to the fact that, at high
362 temperatures and due to the large amount of thermal energy available in the medium, the ratio
363 of energy provided by US over total energy could almost be negligible (Riera et al., 2011).

364 Power US application also affected the convective water transport. As illustrated in **Table**
365 **2**, the application of US increased the k value significantly ($p < 0.05$) at any temperature
366 assayed. The average k increase, compared to nonUS experiments, was 13% and 50% at 30
367 W and 60 W, respectively. US waves create turbulences, oscillating velocities and
368 microstreaming at the interfaces, which leads to a reduction of the boundary layer thickness
369 and so, to an increase in the k values (Puig et al., 2012). Previous works have confirmed the
370 ability of US not only to improve the mass transfer at the interface but also to provoke
371 structural changes on the product surface (Ortuño et al., 2010; Cárcel et al., 2011; Ozuna et
372 al., 2011). For example, from microstructural observations during orange peel drying, Ortuño
373 et al. (2010) observed the spread of waxy compounds over the cuticle surface, which was

374 linked to the great turbulence generated by US at the interface. Therefore, further work will
375 be needed to elucidate how US influences the quality of the material being dried.

376

377 4. Conclusions

378 The results here reported highlight that air-borne ultrasonic application during the
379 convective drying of strawberries is a promising supporting technology to conventional
380 drying processes due to its ability to improve mass transport phenomena, so shortening
381 drying time. The effect of power US on strawberry drying was dependent on the ultrasonic
382 power and temperature applied. Thus, the more the ultrasonic power applied, the faster the
383 drying and the higher the drying temperature, the milder the ultrasonic effect. The modeling
384 pointed to the fact that US application had a significant effect on both the D_e and the external
385 k .

386

387 Acknowledgements

388 This work has been funded by MICINN, Projects Fun-c-Food CSD2007-00063
389 Consolider-INGENIO, DPI2012-37466-C03-03 and Comunidad de Madrid, project
390 ALIBIRD 2009/AGR-1469 and Comunidad Valencia, project PROMETEO/2010/062. J.G.S.
391 also thanks CSIC and the EU for a pre-doctoral JAE grant.

392

393 **Nomenclature**

a_w	Water activity	
C	BET's model parameter	
DM	Dry matter	
D_e	Effective moisture diffusivity	m^2/s
D_0	Pre-exponential Arrhenius factor	
E_a	Activation energy	kJ/mol
k	Mass transfer coefficient	$kg\ W/m^2/s$
L	Mass transport characteristic dimension	m
N	Number of experimental points	
R	Universal gas constant	$kJ/mol/K$
S_w^2	Variance of experimental moisture	$(kg\ W/kg\ DM)^2$
S_{tw}^2	Variance of moisture estimation	$(kg\ W/kg\ DM)^2$
t	Time	s
T	Temperature	K
V	Volume	m^3
VAR	Explained variance	
W	Moisture content	$kg\ W/kg\ DM$
x	Mass transport characteristic direction	
ρ_{ds}	Dry solid density	$kg\ DM/m^3$
φ_{air}	Relative humidity of the drying air	

Subscripts

$calc$	Calculated
exp	Experimental
m	Monolayer
0	Initial
p	Local

395 **References**

- 396 A.O.A.C. (1990). Method N° 934.06. Official Methods of Analysis, Association of Official
397 Analytical Chemists: Arlington, VA.
- 398 Aversa, M., Curcio, S., Calabrò, V., & Iorio, G. (2011). Measurement of the water-diffusion
399 coefficient, apparent density changes and shrinkage during the drying of eggplant
400 (solanum melongena). *International Journal of Food Properties*, 14, 523-537.
- 401 Awad, T.S., Moharram, H.A., Shaltout, O.E., Asker, D., & Youssef, M.M. (2012).
402 Applications of ultrasound in analysis, processing and quality control of food: A
403 review. *Food Research International*, 48, 410-427.
- 404 Barati, E., & Esfahani, J.A. (2013). A novel approach to evaluate the temperature during
405 drying of food products with negligible external resistance to mass transfer. *Journal of*
406 *Food Engineering*, 114, 39-46.
- 407 Blahovec, J., & Yanniotis, S. (2010). GAB generalised equation as a basis for sorption
408 spectral analysis. *Czech Journal of Food Science*, 28, 345-354.
- 409 Bon, J., Rosselló, C., Femenia, A., Eim, V., & Simal, S. (2007). Mathematical Modeling of
410 Drying Kinetics for Apricots: Influence of the External Resistance to Mass Transfer.
411 *Drying Technology*, 25, 1829-1835.
- 412 Brunauer, S., Emmet, P.H., & Teller, E. (1938). Adsorption of gases in multimolecular
413 layers. *Journal of the American Chemical Society*, 60, 309-319.
- 414 Brunauer, S., Deming, L.S., Deming, W.E., & Teller, E. (1940). On a theory of the van der
415 Waals adsorption of gases. *Journal of American Chemistry Society*, 62, 1723-1732.

- 416 Cárcel, J.A., García-Pérez, J.V., Riera, E., & Mulet, A. (2007). Influence of high intensity
417 ultrasound on drying kinetics of persimon. *Drying Technology*, 25, 185-193.
- 418 Cárcel, J.A., Nogueira, R.I., García-Pérez, J.V., Sanjuan, N., & Riera, E. (2010). Ultrasound
419 effects on the mass transfer during drying kinetic of olive leave (*Olea europea*, var.
420 serrana). *Deffect Diffussion Forum*, 297-301, 1083-1090.
- 421 Cárcel, J.A., García-Pérez, J.V., Riera, E., & Mulet, A. (2011). Improvement of convective
422 drying of carrot by applying power ultrasound. Influence of mass load density. *Drying*
423 *Technology*, 29, 174-182.
- 424 Cárcel, J.A., García-Pérez, J.V., Benedito, J., & Mulet, A. (2012). Food process innovation
425 through new technologies: Use of ultrasound. *Journal of Food Engineering*, 110, 200-
426 207.
- 427 Chandrapala, J., Oliver, C, Kentish, S., & Ashokkumar, M. (2012). Ultrasonics in food
428 processing. *Ultrasonic Sonochemistry*, 19, 975-983.
- 429 Chen, X.D., & Mujumdar, A.S. (2008). *Drying Technologies in Food Processing*. Singapore,
430 India.
- 431 Chemat, F., Zill-e-Huma, & Khan, M.K. (2011). Applications of ultrasound in food
432 technology: Processing, preservation and extraction. *Ultrasonic Sonochemistry*, 18,
433 813-835.
- 434 De la Fuente, S., Riera, E., Acosta, V.M., Blanco, A., & Gallego-Juárez, J.A. (2006). Food
435 drying process by power ultrasound. *Ultrasonics*, 44, e523-e527.
- 436 Doymaz, I. (2004). Convective air drying characteristics of thin layer carrots. *Journal of*
437 *Food Engineering*, 61, 359-364.

- 438 Doymaz, I. (2008). Convective drying kinetics of strawberry. *Chemical Engineering and*
439 *Processing*, 47, 914-919.
- 440 Erbas, M., Ertugay, M.F., & Certel, M. (2005). Moisture adsorption behaviour of semolina
441 and farina. *Journal of Food Engineering*, 69, 191-198.
- 442 Gallego-Juarez, J.A. (2010). High-power ultrasonic processing: recent developments and
443 prospective advances. *Physics Procedia*, 3, 35-47.
- 444 Garau, M.C., Simal, S., Femenia, A., & Roselló, C. (2006). Drying of orange skin: Drying
445 kinetics modelling and functional properties. *Journal of Food Engineering*, 75, 288-
446 295.
- 447 García-Noguera, J., Oliveira, F.I.P., Gallao, M.I., Weller, C.L., Rodrigues, S., & Fernandes,
448 F.A.N. (2010). Ultrasound-assisted osmotic dehydration of strawberries: Effect of
449 pretreatment time and ultrasonic frequency. *Drying Technology*, 28, 294-303.
- 450 García-Pérez, J.V., Cárcel, J.A., De la Fuente, S., Riera, E. (2006a). Ultrasonic drying of
451 foodstuff in a fluidized bed. Parametric study. *Ultrasound*, 44, e539-e543.
- 452 García-Pérez, J.V., Roselló, C., Cárcel, J.A., De la Fuente, S., & Mulet, A. (2006b). Effect of
453 air temperature on convective drying assisted by high power ultrasound. *Defect and*
454 *Difussion Forum*, 258-260, 563-574.
- 455 García-Pérez, J.V., Cárcel, J.A., Clemente, G., & Mulet, A. (2008). Water sorption isotherms
456 for lemon peel at different temperaturas and isosteric heats. *LWT-Food Science and*
457 *Technology*, 41, 18-25.

458 García-Pérez, J.V., Cárcel, J.A., Riera, E., & Mulet, A. (2009). Influence of the applied
459 acoustic energy on the drying of carrots and lemon peel. *Drying Technology*, 27, 281-
460 287.

461 García-Pérez, J.V., Ozuna, C., Ortuño, C., Cárcel, J.A., & Mulet, A. (2011). Modelling
462 ultrasonically assisted convective drying of eggplant. *Drying Technology*, 29, (13)
463 1499-1509.

464 García-Pérez, J.V., Ortuño, C., Puig, A., Cárcel, J.A., & Perez-Munuera, I. (2012).
465 Enhancement of water transport and microstructural changes induced by high-
466 intensity ultrasound application on orange peel drying. *Food and Bioprocess*
467 *Technology*, 5, 2256-2265.

468 Giampieri, F., Tulipani, S., Alvarez-Suarez, J.M., Quiles, J.L., Mezzetti, B., & Battino, M.
469 (2012). The strawberry: Composition, nutritional quality and impact on human health.
470 *Nutrition*, 28, 9-19.

471 Giner, S.A. (2009). Influence of Internal and External Resistances to Mass Transfer on the
472 constant drying rate period in high-moisture foods. *Biosystems Engineering*, 102, 90-
473 94.

474 Koc, B., Fren, I., & Kaymak Ertekin, F. (2008). Modelling bulk density, porosity and
475 shrinkage of quince during drying: The effect of drying method. *Journal of Food*
476 *Engineering*, 85, 340-349.

477 Li, Z.Y., Wang, R.F., & Kudra, T. (2011). Uniformity Issue in microwave drying. *Drying*
478 *Technology*, 29, 652-660.

479 Lim, L., Tang, J., & He, J. (1995). Moisture sorption characteristics of freeze dried
480 blueberries. *Journal of Food Science*, 60, 810-814.

481 Mäskan, M., & Göğüs, F. (1998). Sorption isotherms and drying characteristics of mulberry
482 (Morus alba). *Journal of Food Engineering*, 37, 437-449.

483 Molina Filho, L., Gonçalves, R., Karla, A., Mauro, M.A., & Frascareli, E.C. (2011). Moisture
484 sorption isotherms of fresh and blanched pumpkin (Curcubita moschata). *Ciência e*
485 *Tecnologia de Alimentos*, 31, 714-722.

486 Moraga, G., Martínez-Navarrete, N., & Chiralt, A. (2004). Water sorption isotherms and
487 glass transition in strawberries: influence of pretreatment. *Journal of Food*
488 *Engineering*, 62, 315-321.

489 Mulet, A., Blasco, M., García-Reverter, J., & García-Pérez, J.V. (2005). Drying kinetics of
490 *Curcuma longa* rhizomes. *Journal of Food Science*, 7, e318-e323.

491 Ortuño, C., Pérez-Munuera, I., Puig, A., Riera, E., & García-Pérez, J.V. (2010). Influence of
492 power ultrasound application on mass transport and microstructure of orange peel
493 during hot air drying. *Physics Procedia*, 3, 153-159.

494 Ozuna, C., Cárcel, J.A., García-Pérez, J.V., & Mulet, A. (2011). Improvement of water
495 transport mechanisms during potato drying by applying ultrasound. *Journal of the*
496 *Science of Food and Agriculture*, 91, 2511-2517.

497 Puig, A., Perez-Munuera, I., Cárcel, J.A., Hernando, I., & García-Pérez, J.V. (2012).
498 Moisture loss kinetics and microstructural changes in eggplant (*Solanum melongena*
499 *L.*) during conventional and ultrasonically assisted convective drying. *Food and*
500 *Bioproducts Processing*, 90, 624-632.

501 Ramallo, L.A., & Mascheroni, R.H. (2013). Effect of shrinkage on prediction accuracy of the
502 water diffusion model for pineapple drying. *Journal of Food Process Engineering*, 36,
503 66-76.

504 Rastogi, N.K. (2012). Recent developments in infrared heating in food processing. *Critical*
505 *Reviews in Food Science and Nutrition*, 52, 737-760.

506 Riera, E., García-Pérez, J.V., Cárcel, J.A., Acosta, V., & Gallego-Juárez, J.A. (2011).
507 Computational study of ultrasound-assisted drying of food materials. En: Knoerzer,
508 K., Juliano, P., Roupas, P., Versteeg, C. (Eds.). *Innovative Food Processing*
509 *Technologies: Advances in Multiphysics Simulation*. Ed. IFT Press and John Wiley &
510 Sons Ltd.

511 Sablani, S.S., & Rahman, M.S. (2008). Fundamentals of Food Dehydration. In: *Food Drying*
512 *Science and Technology. Microbiology, Chemistry, Applications*. Ed. By Hui, Y.H.,
513 Clary, C., Farid, M.M., Fasina, O.O., Noomhorm, A. and Welti-Chanes, J. DEStech
514 Publications, Inc. Lancaster, USA.

515 Schössler, K., Jäger, H., & Knorr, D. (2012). Effect of continuous and intermittent ultrasound
516 on drying time and effective diffusivity during convective drying of apple and red bell
517 pepper. *Journal of Food Engineering*, 108, 103-110.

518 Senadeera, W., Bhandari, B.R., Young, G., & Wijesinghe, B. (2003). Influence of shapes of
519 selected vegetable materials on drying kinetics during fluidized bed drying. *Journal of*
520 *Food Engineering*, 58, 277-283.

521 Simal, S., Femenia, A., García-Pascual, P., & Rosselló, C. (2003). Simulation of the drying
522 curves of a meat-based product: Effect of the external resistance to mass transfer.
523 *Journal of Food Engineering*, 58, 193-199.

- 524 Simal, S., Femenia, A., Cárcel, J.A., & Rosselló, C. (2005). Mathematical modelling of the
525 drying curves of kiwi fruits: Influence of the ripening stage. *Journal of the Sciences of*
526 *Food and Agriculture*, 85, 425-432.
- 527 Soria, A.C., & Villamiel, M. (2010). Effect of ultrasound on the technological properties and
528 bioactivity of food: a review. *Trends in Food Science and Technology*, 21, 323-331.
- 529 Vázquez, G., Chenlo, F., Moreira, L., & Carballo, L. (1999). Desorption isotherms of
530 muscatel and aledo grapes, and the influence of pretreatments on muscatel isotherms.
531 *Journal of Food Engineering*, 39, 199-205.
- 532 Vega-Gálvez, A., & Lemus-Mondaca, R. (2006). Modelado de la cinética de secado de la
533 papaya chilena (*Vasconcellea pubescens*). *Información Tecnológica*, 17, 23-31.
- 534 Vega-Gálvez, A., Miranda, M., Bilbao-Sáinz, C., Uribe, E., & Lemus-Mondaca, R. (2008).
535 Empirical modeling of drying process for Apple (cv. *Granny Smith*) slices at different
536 air temperatures. *Journal of Food Processing and Preservation*, 32, 972-986.
- 537 Vega-Gálvez, A., López, J., Miranda, M., Di Scala, K., Yagnam, F., & Uribe, E. (2009).
538 Mathematical modelling of moisture sorption isotherms and determination of isosteric
539 heat of blueberry variety O'Neil. *International Journal of Food Science and*
540 *Technology*, 44, 2033-2041.
- 541 Wu, L., Orikasa, T., Ogawa, Y., & Tagawa, A. (2007). Vacuum drying characteristics of
542 eggplant. *Journal of Food Engineering*, 83, 422-429.
- 543 Yu, L., Mazza, G., & Jayas, D.S. (1998). Moisture sorption characteristics of freeze-dried,
544 osmo-freeze-dried, and osmo-air-dried cherries and blueberries. *Transactions of the*
545 *ASAE*, 42, 141-147.

547 **FIGURE CAPTIONS**

548 **Figure 1** Diagram of the ultrasonic assisted drier. 1. Fan, 2. Heating unit, 3. Anemometer, 4.
549 Three-way valve, 5. Thermocouple, 6. Sample loading chamber, 7. Coupling material, 8.
550 Pneumatic system, 9. Ultrasonic transducer, 10. Vibrating cylinder, 11. Trays, 12. Balance,
551 13. Impedance matching unit, 14. Digital power meter, 15. High power ultrasonic generator,
552 16. PC.

553 **Figure 2** Drying kinetics (2 m/s) of strawberry slabs at different temperatures applying
554 different ultrasonic powers.

555 **Figure 3** Variation of volume and moisture ratio for strawberry cubes during drying (2 m/s,
556 70 °C).

557 **Figure 4** Experimental and calculated (BET model) sorption isotherm of strawberry samples
558 at 25 °C.

559 **Figure 5** Experimental (W_{exp}) vs. calculated (W_{calc}) moisture content of strawberry slabs
560 dried at 70 °C applying an ultrasonic power of 0, 30 and 60 W.

561 **Figure 6** Fit of Arrhenius equation (continuous line) to the identified moisture diffusivities
562 for power-ultrasound assisted strawberry drying. Experiments carried out at 2 m/s applying
563 different ultrasonic powers (0, 30 and 60 W).

564

Figure 1

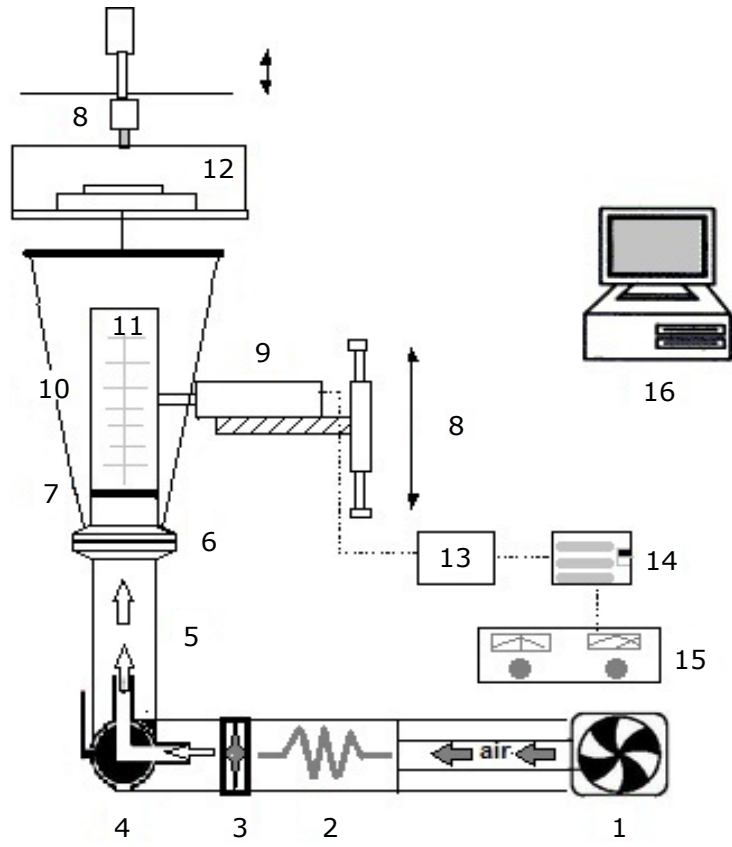


Figure 2

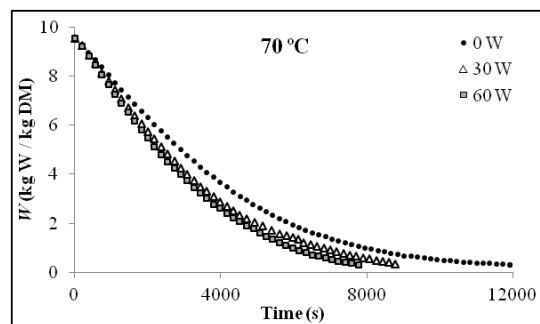
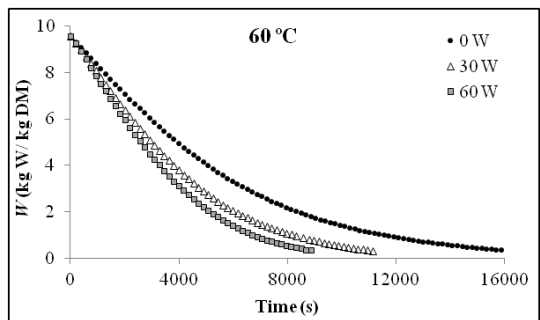
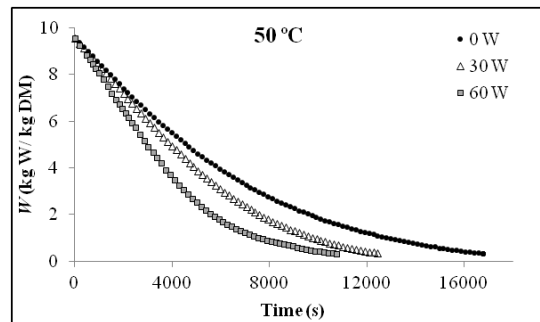
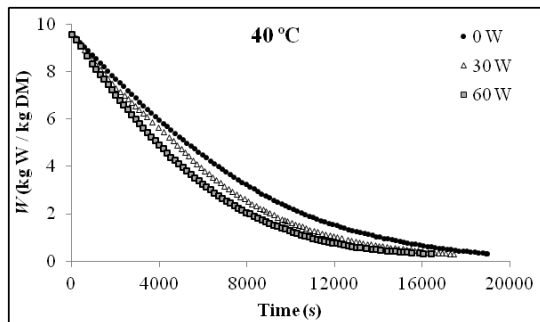


Figure 3

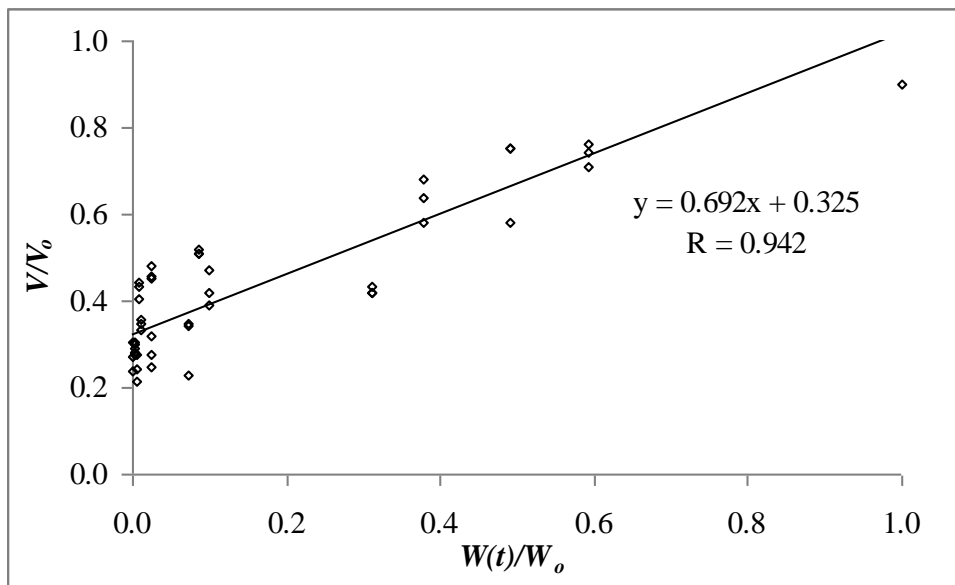


Figure 4

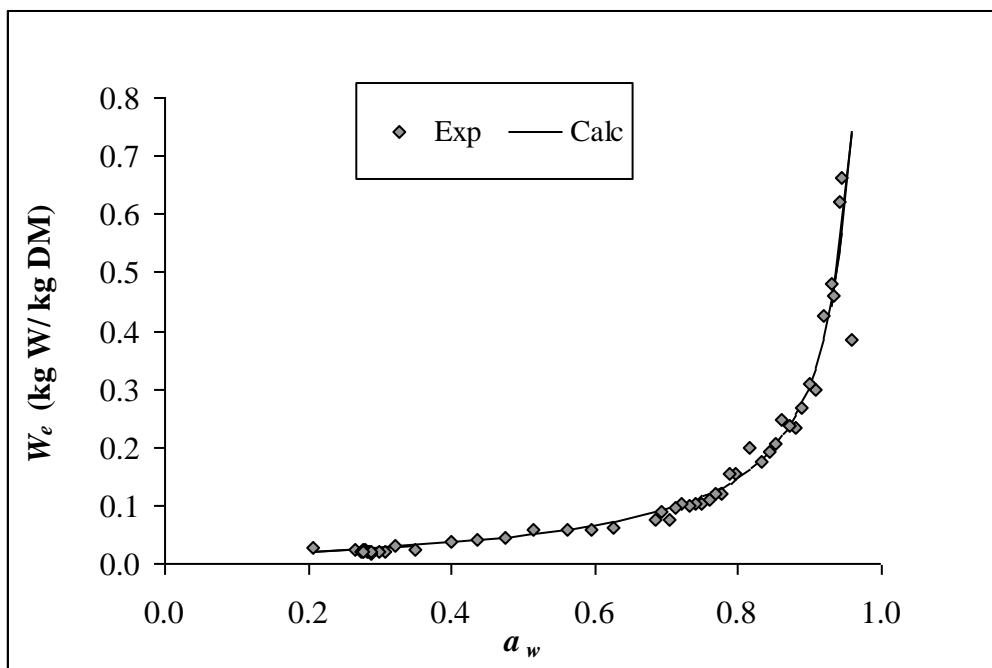


Figure 5

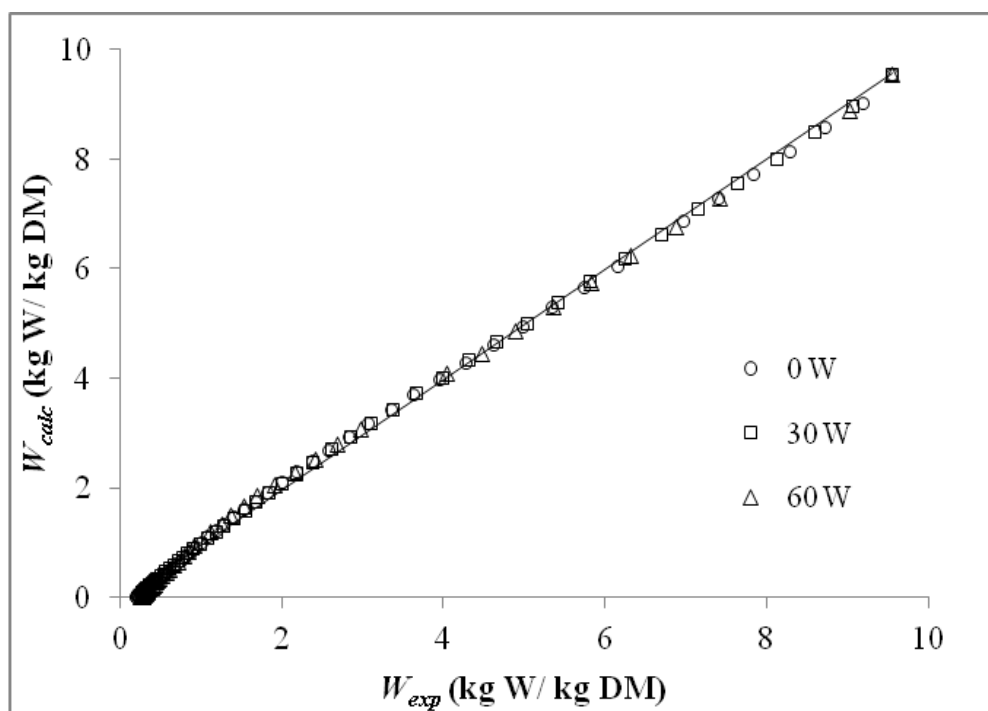


Figure 6

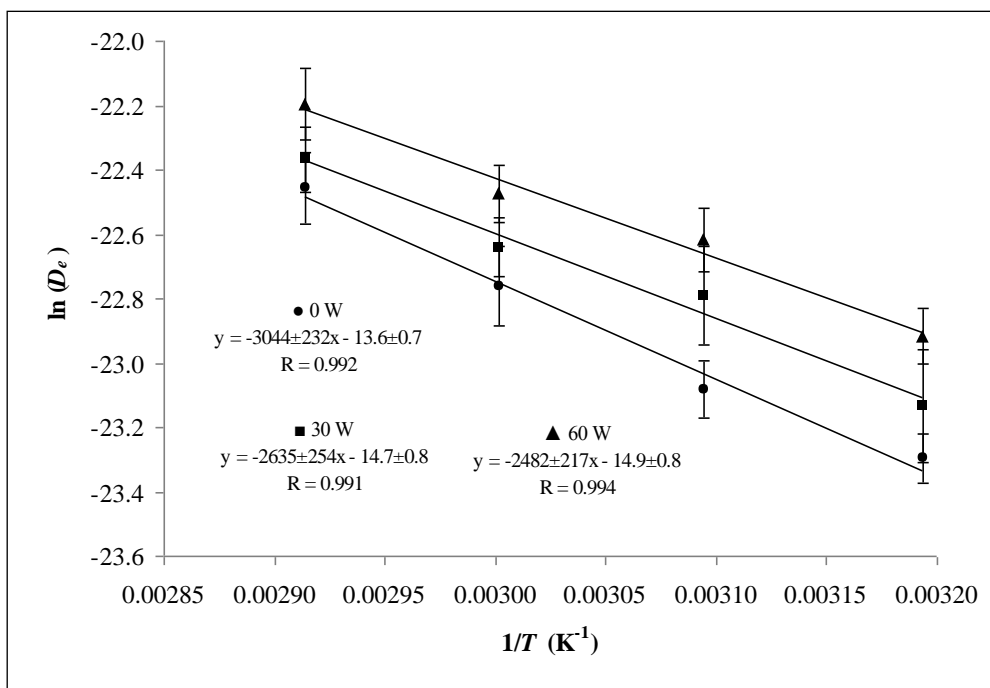


Table 1 Processing conditions for ultrasonically assisted convective drying of strawberries

Assays	Temperature (°C)	US power* (W)
nonUS-40	40	0
US-40-30	40	30
US-40-60	40	60
nonUS-50	50	0
US-50-30	50	30
US-50-60	50	60
nonUS-60	60	0
US-60-30	60	30
US-60-60	60	60
nonUS-70	70	0
US-70-30	70	30
US-70-60	70	60

*Specific electric power applied to the transducer.

Table 2 Modeling of drying kinetics of ultrasonically assisted drying of strawberry. Identified parameters and statistical analysis (Means \pm SD)

<i>Assays</i>	D_e ($10^{-10}m^2/s$)	k ($10^{-5}kg W/m^2/s$)	<i>VAR</i> (%)	<i>MRE</i> (%)
nonUS-40	0.763 \pm 0.075 ^a	1.446 \pm 0.256 ^a	99.74	3.79
US-40-30	0.898 \pm 0.173 ^{ab}	1.380 \pm 0.405 ^a	99.98	3.30
US-40-60	1.117 \pm 0.086 ^{bc}	1.633 \pm 0.160 ^{ab}	99.97	3.26
nonUS-50	0.947 \pm 0.089 ^{ab}	1.630 \pm 0.194 ^{ab}	99.97	4.25
US-50-30	1.267 \pm 0.154 ^{cd}	1.750 \pm 0.311 ^{abc}	99.90	4.23
US-50-60	1.500 \pm 0.099 ^{de}	2.017 \pm 0.180 ^{bcd}	99.97	3.84
nonUS-60	1.305 \pm 0.123 ^{cd}	2.008 \pm 0.234 ^{bcd}	99.85	4.09
US-60-30	1.470 \pm 0.091 ^{def}	2.380 \pm 0.150 ^{cde}	99.99	1.06
US-60-60	1.737 \pm 0.089 ^{efg}	2.593 \pm 0.170 ^{de}	99.98	2.98
nonUS-70	1.772 \pm 0.112 ^{fg}	2.868 \pm 0.202 ^{ef}	99.89	6.75
US-70-30	1.937 \pm 0.101 ^g	3.277 \pm 0.509 ^f	99.93	4.67
US-70-60	2.293 \pm 0.110 ^h	3.387 \pm 0.320 ^f	99.88	3.55

¹Means with the same superscript letter (a-f) within the same column showed no statistically significant differences for their mean values at the 95% confidence level (LSD).